THE USE OF TWO SPACED RADARS TO MEASURE METEOR DRIFTS

K. A. Karimov, V. V. Sidorov

ABSTRACT. Radar was used in Frunze in 1964-1965 to study meteors in order to evaluate the accuracy of wind parameters measured in the meteor region of the atmosphere for small samples and unknown altitudes, as well as to evaluate the effect of using different space and time averaging methods on the accuracy of results obtained.

The investigations covered the 18-month period of observations in the /21
International Year of the Quiet Sun program. They were made using two simultaneously operating radars, spaced 200 km apart in longitude, the antennas of which illuminated the same general region of the atmosphere, or regions spaced up to 500 km apart. The averaged wind characteristics, as obtained by the two radars 200 km apart, were compared. This spacing obviously is not significant from the geophysical point of view (the local time differs by 10 min), but in this case, the possibility of working with common meteors is, for all practical purposes, eliminated, so, independent samples of drift velocities can be obtained.

All published information on wind characteristics in the meteor zone was obtained under the assumption that the averaged wind characteristics do not vary over distances of the order of 300 to 500 km. This position requires experimental verification, however. Hence, the natural question is how quickly do averaged wind characteristics change with longitude, and what is the connection between this and the region of averaged individual measurements?

Equipment and Observation Procedure

Measurements of the drifts of meteor trails were made using specially built radar and the coherent pulse method at a frequency of 39.5 MHz. The /22
frequency of the second radar was shifted 4-5 bandwidths with respect to the first. Reception and transmission were accomplished with a system of two five-element broadside antennas of the "wave channel" type, with a pattern width in the horizontal plane of 25° at the 3 db level. Transmitter power (autooscillator) was 50 kW, the pulse repetition frequency was 100 pps,

the main pulse width was 10 μsec, and the sensitivity of the receivers was $5 \cdot 10^{-14}$ W when the bandwidth of the receivers was 100 kHz. Phase synchronization of the reference oscillator was accomplished by locking onto the frequency of the receiver oscillator. A detailed description of the equipment used is given in reference [1].

The observations included four variants to explain differences in measured wind parameters.

Variant 1. The same component of the wind velocity was observed in the same region of the atmosphere, but the antennas were oriented in opposite directions (Figure 1a).

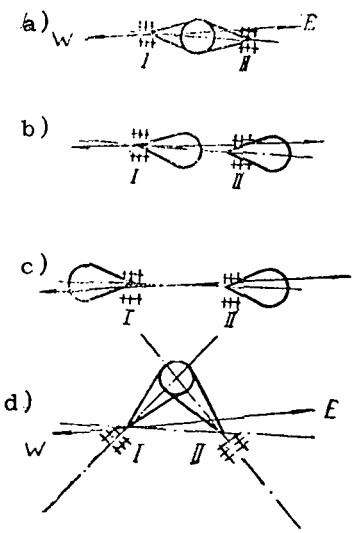

Figure 1. Variants in relative orientations of the antennas for the two radars.

Variant 2. The same wind component was observed with the antennas oriented in the same direction, but in different atmospheric regions (Figure 1b).

Variant 3. Observations were made with opposing antenna orientations and in different regions (Figure 1c).

Variant 4. Observations were made in the same "local" region with simultaneous measurements of two wind components (Figure 1d).

Wind data were processed by an M-20 electronic computer, with allowances made for the statistical weight of each mean hourly velocity. Results were processed primarily in terms of underdense trails. The mean daily number of meteor echoes suitable for measuring Doppler characteristics was of the order of 500.

Results of the Experiments

A good correlation of hourly values of drift velocity ($R > 0.85$) was found for Variant 1 observations, when the same wind velocity component was measured in the same region of the atmosphere (data based on the results of four observation cycles in different months). /24

TABLE I *

Month	Station	Type of equation
January	SOM-I	0,5±1,2 + (9,2±2,4) Sin 15 (t+ 6,4) + (10,8± 2,2) Sin 30 (t+ 4,2) + (4,6±1,9) Sin 45 (t+5,8)
	SOM-II	2,9±2,0 + (6,9±3,3) Sin 15 (t+ 9,3) + (12,7± 3,1) Sin 30 (t+ 4,5) + (9,1±2,8) Sin 45 (t+5,9)
	I, II	1,7±1,8 + (5,9±2,9) Sin 15 (t+ 7,4) + (11,6± 2,8) Sin 30 (t+ 4,4) + (7,1±2,2) Sin 45 (t+5,4)
February	SOM-I	7,5+1,4 + (4,0±2,2) Sin 15 (t+20) + (7,1± 2,0) Sin 30 (t+ 2,1) + (1,9+1,9) Sin 45 (t+3,8)
	SOM-II	4,7±2,2 + (2,9±3,8) Sin 15 (t+15) + (9,4± 3,7) Sin 30 (t+ 1,2) + (5,4±3,0) Sin 45 (t+5,1)
	I, II	6,1±1,8 + (1,4±2,5) Sin 15 (t+20,1) + (7,6± 2,2) Sin 30 (t+ 1,6) + (3,4+2,5) Sin 45 (t+5,4)
March	SOM-I	7,9±1,8 + (9,1±2,6) Sin 15 (t+13,0) + (8,9± 3,0) Sin 30 (t+ 4,8) + (3,7±1,7) Sin 45 (t+0,7)
	SOM-II	7,3+2,3 + (5,9±5,0) Sin 15 (t+12,0) + (11,8± 4,9) Sin 30 (t+ 5,2) + (5,8±3,6) Sin 45 (t+2,4)
	I, II	7,6±2,0 + (8,3±3,5) Sin 15 (t+12,9) + (9,7± 3,0) Sin 30 (t+ 5,1) + (2,0±2,0) Sin 45 (t+2,1)
November	SOM-I	8,3±1,6 + (3,8±2,9) Sin 15 (t+21) + (13± 3,2) Sin 30 (t+ 2,9) + (3,4±2,6) Sin 45 (t+0,8)
	SOM-II	5,8±2,1 + (4,6±2,8) Sin 15 (t+23) + (15,5±2,8) Sin 30 (t+ 2,2) + (3,9±3,0) Sin 45 (t±2,2)
	I, II	7,2±1,9 + (4,7±2,5) Sin 15 (t+12) + (14,1± 3,1) Sin 30 (t+ 3,2) + (2,7±2,2) Sin 45 (t±1,8)

* Commas represent decimal points.

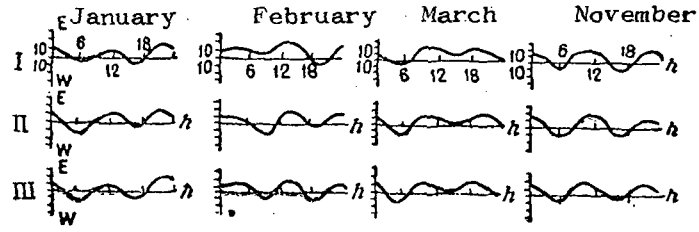

Figure 2. Histograms of drift velocities for Variant 1 observations, as shown in Figure 1a.

Figure 2 shows and Table 1 lists histograms and equations for the corresponding averaged hourly histograms of drift velocities for four months of observations by the two radars for Variant 1 observations, as well as the summed value for the two radars. All subsequent results are reduced to simultaneous observations. /25

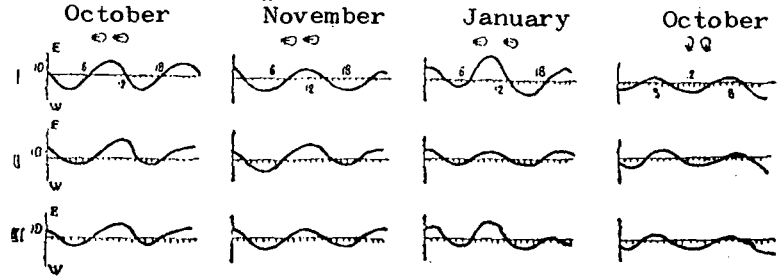

Figure 3. Histograms of drift velocities for Variant 2 observations, as shown in Figure 1b.

The second series of experiments was devoted to an explanation of the dependence of the effect of dispersion of regions of averaging on the measured parameters of the regular wind.

Table 2 lists and Figure 3 shows equations for averaged hourly drift velocity histograms and a summed histogram for the region of averaging of up to 300 km for Variant 2 observations, when the same wind component was measured with identical antenna orientations, but for regions separated by 200 km (conducted for four measurement cycles in different months). /26

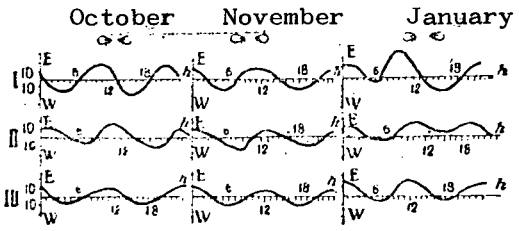

Figure 4. Histograms of drift velocities for Variant 3 observations, as shown in Figure 1c.

Table 3 lists, and Figure 4 shows, equations of averaged hourly drift velocity histograms and summed histograms for the averaging region up to 600 km for 3rd Variant observations, with opposing antenna orientations for regions 500 km apart (three measurement cycles in different months). The question of whether these differences are real values, or simply errors in the observation procedure, requires further study. In the results presented here, however, the A_0 values measured in the regions over the Issyk-Kul' area are systematically higher than over northwestern Kirghizia. It is /27 interesting to note that within area spacings up to 500 km, the daily harmonics appear to be close to opposite in phase, and almost cancel out when averaged in a common zone, so that relative differences appear to be greater. The substantial second harmonic phase shifts (beyond the limits of measurement error) determine the relatively great differences in the amplitudes of the corresponding harmonics.

The summed differences for the set of mean hourly drift velocity values for the two radars can be estimated from the first correlation moment. The corresponding correlation function was calculated for a closed daily cycle with a time shift.

TABLE 2 *

Month	Station	Type of equation
October	SOM-I	— 5,1± 2,2+(4,0± 2,6) Sin 15 (*t*+21,6) + (10,3± 2,8) Sin 30 (*t*+ 9,0) + (4,8± 2,1) Sin 45 (*t* + 5,5)
	SOM-II	— 7,0± 2,0+(7,2± 3,0) Sin 15 (*t*+20,6) + (12,7± 3,0) Sin 30 (*t*+ 8,5) + (4,2± 3,4) Sin 45 (*t*+ 5,8)
	I, II	— 6,0±1,9+(5,5± 2,5) Sin 15 (*t*+21,3) + (11,6± 2,6) Sin 30 (*t*+ 8,8) + (4,5± 3,2) Sin 45 (*t* + 5,6)
October	SOM-I	0,9± 2,8+(1,3± 2,9) Sin 15 (*t*+ 7,2) + (21,3± 4,0) Sin 30 (*t*+ 4,9) + (3,6± 4,0) Sin 45 (*t* + 6,3)
	SOM-II	7,7± 2,3+(1,8± 2,2) Sin 15 (*t*+12,7) + (12,7± 3,2) Sin 30 (*t*+ 2,9) + (2,2± 3,2) Sin 45 (*t* + 4,9)
	I, II	4,3± 2,0+(5,5± 2,1) Sin 15 (*t*+ 7,5) + (15,0± 3,0) Sin 30 (*t*+ 4,3) + (2,5± 2,8) Sin 45 (*t* + 5,7)
November	SOM-I	— 0,8± 1,6+(3,4± 2,6) Sin 15 (*t*+19,2) + (11,0± 3,0) Sin 30 (*t*+ 2,8) + (5,4± 2,6) Sin 45 (*t* + 1,6)
	SOM-II	6,0± 2.2+(7,0± 3,8) Sin 45 (*t*+ 16,2) + (15,5± 3,5) Sin 30 (*t*+ 2,1) + (3,8± 3,0) Sin 45 (*t* + 1,9)
	I, II	2,7± 1,9+(5,4± 2,5) Sin 15 (*t*+ 17,4) + (14,6± 3,0) Sin 30 (*t*+ 3,4) + (4,3± 3,0) Sin 45 (*t* + 1,7)
January	SOM-I	6,2± 1,8+(2,5± 2,2) Sin 15 (*t*+ 8,6) + (10,8± 2,6) Sin 30 (*t*+ 4,6) + (4,4± 3,5) Sin 45 (*t* + 5,6)
	SOM-II	11,8± 2,1+(5,1± 2,8) Sin 15 (*t*+ 11,1) + (6,3± 2,5) Sin 30 (*t*+ 2,4) + (0,9± 2,9) Sin 45 (*t* + 2,7)
	I, II	9,4± 1,8+(2,9± 2,3) Sin 15 (*t*+ 9,5) + (6,9± 2,4) Sin 30 (*t*+ 3,0) + (5,6± 3,3) Sin 45 (*t* + 7,6)

* Commas represent decimal points.

TABLE 3 *

Month	Station	Type of equation
October	SOM-I	0,9± 2,8 + (1,3± 2,9) Sin 15 (*t* + 7,2) + (21,3± 4,0) Sin 30 (*t*+4,9) + (3,6±4,0) Sin 45 (*t* + 6,3)
	SOM-II	4,7± 2,1 + (6,1± 3,0) Sin 15 (*t* +22,9) + (17,4± 3,8) Sin 30 (*t*+2,3) + (5,0±3,8) Sin 45 (*t* + 1,9)
	I, II	2,8± 2,0 + (2,1± 2,8) Sin 15 (*t* + 0,4) + (6,3± 3,1) Sin 30 (*t*+5,5) + (6,4±3,8) Sin 45 (*t* + 4,0)
November	SOM-I	— 0,8± 1,6 + (3,5± 2,6) Sin 15 (*t* +19,2) + (14,8± 3,6) Sin 30 (*t*+3,0) + (5,6±2,8) Sin 45 (*t* + 1,6)
	SOM-II	— 3,8± 1,9 + (3,6 ± 2,6) Sin 15 (*t* + 7,9) + (12,6± 3,8) Sin 30 (*t*+1,8) + (10±5,0) Sin 45 (*t* + 5,9)
	I, II	— 2,4± 1,8 + (0,6± 2,5) Sin 15 (*t* +23,0) + (12,1± 3,3) Sin 30 (*t*+2,3) + (2,6±3,2) Sin 45 (*t* + 1,5)
January	SOM-I	7,8± 2,0 + (10,7 ± 4,8) Sin 15 (*t* +22,7) + (22,3± 5,0) Sin 30 (*t*+3,8) + (9,8±4,5) Sin 45 (*t* + 7,2)
	SOM-II	11,8± 1,9 + (5,1± 3,9) Sin 15 (*t* +11,1) + (6,3± 3,5) Sin 30 (*t*+2,4) + (0,9±4,0) Sin 45 (*t* + 2,7
	I, II	9,8± 1,8 + (2,6± 3,6) Sin 15 (*t* +22,4) + (14,3± 3,3) Sin 30 (*t*+3,7) + (4,3±3,6) Sin 45 (*t* + 7,2)

* Commas represent decimal points.

The normalized correlation coefficient was calculated using the formula

$$r(T_\kappa) = \frac{\sum_{i=1}^{n} n_{uv} u_i v_{i+\kappa} - n\bar{u}\,\bar{v}}{\left[\left(\sum_{i=1}^{n} n_u\, u_i - n\bar{u}\right)^2 \left(\sum_{i=1}^{n} n_v v_i - n\bar{v}\right)^2\right]^{1/2}},$$

where

n is the number of intervals in the days;

n_{uv} is the weight function;

$u_i v_{i+k}$ is the wind velocity correlating value for the i^{th} and $i+k^{th}$ intervals.

The scantiness of the sample led to a random, rather than a systematic, error in the statistical wind characteristic values. The root-mean-square error in the normalized correlation function attributable to this factor was estimated by using the formula /28

$$\sigma_r = \frac{1-r^2}{\sqrt{n-1}},$$

where

r is the correlation coefficient;

n is sample volume.

Analysis of the correlation curves reveals that the correlation coefficient falls to 0.7, on the average, with a shift in the correlation maximum of the order of one hour, when the separation in the working areas is 200 km in longitude. The correlation at coinciding times falls to 0.3, and the shift in the correlation maximum increases to 1.5 hours, when the separation between areas is increased to 500 km.

Figure 5a shows the decrease in wind measurement correlation with increase in separation between measurement areas.

Figure 5b shows the curve indicating an increase in the time shift to the correlation maximum with increase in separation between areas. The dashed line is the curve incorporating the correction for local time. The effect of a systematic lag in the 12-hour harmonic for the eastern region with respect to western of 1.5 hours when operating areas were 500 km apart was unexpected. The fixed phase position of the 12-hour harmonic for the /29

first radar consistently occurs earlier than for the second. The second radar was to the east of the first. Characteristic of all the correlation curves is the occurrence of the correlation maximum to the right (the ordinates of the second radar were fixed for the correlation function calculations, and the values of the ordinates of the first were shifted to the time increase side).

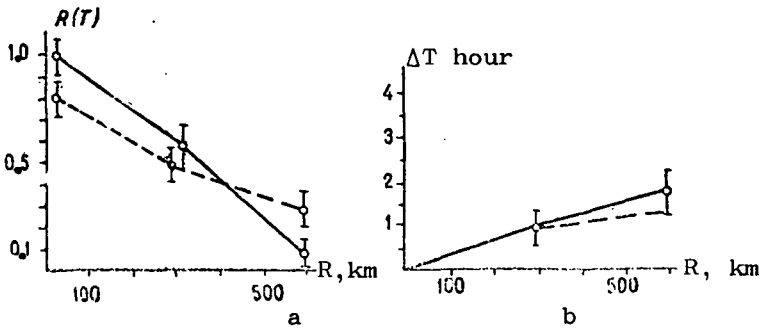

Figure 5. a - correlation of mean hourly wind velocities at two radars in terms of separation between areas; b - time shift to correlation maximum in terms of distance between sounded regions.

The phases of the 12-hour wind velocity oscillations at the first radar consistently led the corresponding phases at the second, as is evident from the above harmonic resolution equations.

The results indicate extraordinarily sharp longitudinal changes in regular wind parameter not previously noted. It is possible that the phase leads noted are among the effects associated with the existence of the hydrodynamic waves suggested by Hines [2] as being present in the E region of the ionosphere.

The experimental data obtained do not permit a final decision to be made with respect to whether these changes are wave, or random, in nature, or to what sort of spatial periodicity there is to the phase shifts noted. However, the results obtained indicate the incorrectness of the method conventionally used to measure mean velocity vectors by measuring the zonal and meridional components of one radar in different areas.

Simultaneous Measurement of the Zonal and Meridional Components of the Wind Velocity Vector by Two Radars In One Area

Observations made using Variant 4 (five measurement cycles were used in different months), and comparison of these data with results obtained using the generally accepted procedure, showed that the transition to one measurement area eliminated many previously observed, and difficult to explain, phenomena of the type that skew the axes of the polar diagrams characterizing the 12-hour changes in the velocity vector.

Table 4 lists, and Figure 6 shows, the equations for the mean curves for the harmonic resolution of the hourly histograms of wind velocities for conventional measurements (the results from one radar) and the measurements for one "local" area by the two radars from May to September 1965.

TABLE 4 *

Month	Radar and bearing	Type of equation
May	I	53° — 1,7+ 2,75 Sin 15 (t +14,0)+ 18,5 Sin 30 (t+ 6,33)+ 3,2 Sin 45 (t +2,6)
		323° + 4,4 +11,6 Sin 15 (t+ 3,86)+ 8,7 Sin 30 (t+ 3,56)+ 6,7 Sin 45 (t +0,76)
	II	323° +14,5 + 9,87 Sin 15 (t+ 7,3)+ 18,0 Sin 30 (t+ 4,0)+ 4,9 Sin 45 (t +6,84)
June	I	53° — 0,8 + 9,6 Sin 15 (t +20,9)+ 24,8 Sin 30 (t+ 7,27)+ 7,1 Sin 45 (t +4,97)
		323° + 5,3 + 8,8 Sin 15 (t + 1,96)+ 7,5 Sin 30 (t+ 4,01)+ 9,6 Sin 45 (t +0,01)
	II	323° +11,3 +14,7 Sin 15 (t + 3,0)+ 22,9 Sin 30 (t+ 4,12)+ 7,4 Sin 45 (t +7,52)
July	I	53° + 4,0 + 9,52 Sin 15 (t + 0,3)+ 17,3 Sin 30 (t+ 7,3)+ 5,1 Sin 45 (t +1,17)
		323° +13,5 + 9,96 Sin 15 (t + 1,3)+ 17,94 Sin 30 (t+ 1,22)+ 6,5 Sin 45 (t +4,6)
	II	323° +16,9 +10,8 Sin 15 (t + 1,8)+ 8,2 Sin 30 (t+ 2,85)+ 8,4 Sin 45 (t +7,44)
August	I	53° + 4,0 +10,7 Sin 15 (t +22,7)+ 11,09 Sin 30 (t+ 7,28)+ 8,7 Sin 45 (t +5,47)
		323° +24,1+12,8 Sin 15 (t +23,4)+ 23,9 Sin 30 (t+ 5.4)+ 4,6 Sin 45 (t +4,5)
	II	323° + 1,0 + 6,0 Sin 15 (t + 9,98)+ 14,8 Sin 30 (t+4,56)+1,58 Sin 45 (t +3,57)
September	I	53° + 1,4 + 0,33 Sin 15 (t +19,3)+ 9,9 Sin 30 (t+ 8,61)+10,2 Sin 45 (t +3,4)
		323° — 4,2 +11,5 Sin 15 (t + 3,4)+ 12,8 Sin 30 (t+ 3,91)+10,4 Sin 45 (t +1,42)
	II	323° + 1,1 + 1,92 Sin 15 (t+ 10,9)+ 12,9 Sin 30 (t+ 4,58)+ 5,63 Sin 45 (t +4,12)

* Commas represent decimal points.

Listed on line I are the mean hourly velocity histogram equations /31
for the first radar when antenna orientation was northeast (azimuth 53°) and northwest (azimuth 323°). Listed on line II are the mean hourly wind velocity histogram equations for the second radar when antenna orientation was northwest (azimuth 323°). The initial measurements were of the "local" type when the antenna of the first radar was pointed to the northeast, and that of the second (located 200 km to the westward of the first) to the northwest. Antenna radiation pattern conditions were selected to illuminate a

single meteor region in the atmosphere, and the angle between the mean hourly values of the horizontal components of the wind velocity was 90°.

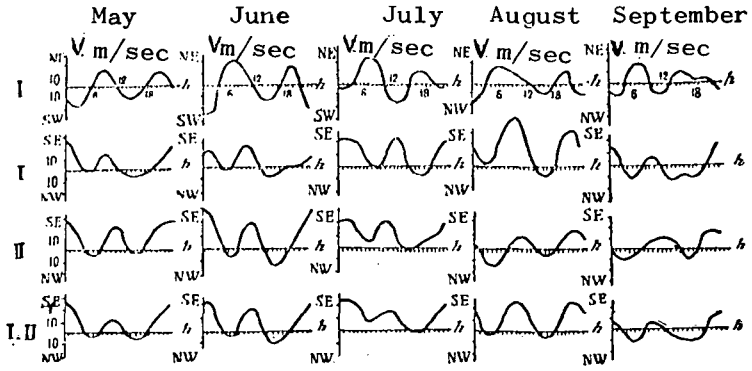

Figure 6. Histogram of drift velocities for the 4th (d) observation variant.

After three to five days of this type of measurements the antennas of the first radar were rotated 90° to the original bearing, and the second component of the wind velocity vector, which had been measured earlier by the second radar, was measured, but this time in an area 200 km away (measurements ceased at the second radar).

Figure 7 shows the polar diagrams of the 24-hour A_1 and the 12-hour A_2 harmonics.

The shift in phases between the north and west bearings differs substantially from 90° (3 hours) in the case of the 12-hour components for conventional measurements (series 1). Comparisons will show that in the majority of cases the major axes of the ellipses of the polar diagrams are oriented N-S and E-W when working the same area, despite the fact that the antennas were oriented NE and NW. The difference in phases between the north and east components, measured by two radars in the same area, was /33 much closer to 3 hours for the 12-hour component than for the observations made by one radar.

The mean deviation of the major axes from north, for all months, based on "local" measurements, was $\Delta\varphi = \pm 0.5$ hr, which agrees well with the mean error in the phase measurement for the 12-hour component. This mean deviation was $\Delta\alpha = \pm 1.5$ hr for conventional single-radar measurements.

The presence of some divergence in measured values of the prevailing

wind at two radars for measurements of the same component can be attributed to measurements having been made on noncoincident days.

The abrupt shifts in the prevailing wind from day to day (not associated with statistics) that we had previously noted made observations of the zonal and meridional components difficult on noncoincident days, so it is desirable to take measurements by switching the antennas to two azimuths, or to use two radar installations in a "local" variant and simultaneously measure two wind components.

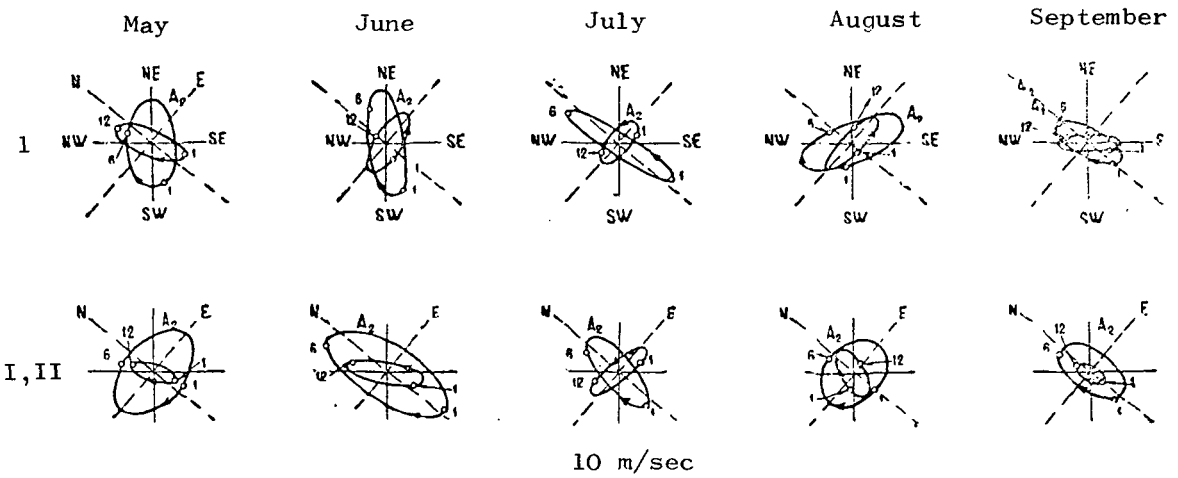

Figure 7. Polar diagrams of the 24-hour A_1 and 12-hour A_2 wind velocity component vectors for conventional (1) and two-radar (I, II) measurements.

REFERENCES

1. Karimov, K. A., Kostromin, V. D., Berezovskiy, M. I., "The Radar Installation for Observing Meteors in Kirghizia," Sb. Meteornoye rasprostraneniye radiovoln [In collection: Meteor Radio Wave Propagation], Part 3-4, Kazan', 1966.

2. Hines, C. O., "An Interpretation of Certain Ionospheric Motions in Terms of Atmospheric Waves," J. Geophys. Res., Vol. 64, No. 12, 1959.